

# Surveilling and Tracking COVID-19 Patients Using a Portable Quantum Dot Smartphone Device

Yuwei Zhang,<sup>□</sup> Ayden Malekjahani,<sup>□</sup> Buddhisha N. Udugama, Pranav Kadhiresan, Hongmin Chen, Matthew Osborne, Max Franz, Mike Kucera, Simon Plenderleith, Lily Yip, Gary D. Bader, Vanessa Tran, Jonathan B. Gubbay, Allison McGeer, Samira Mubareka, and Warren C. W. Chan\*



Cite This: *Nano Lett.* 2021, 21, 5209–5216



Read Online

ACCESS |



Metrics & More



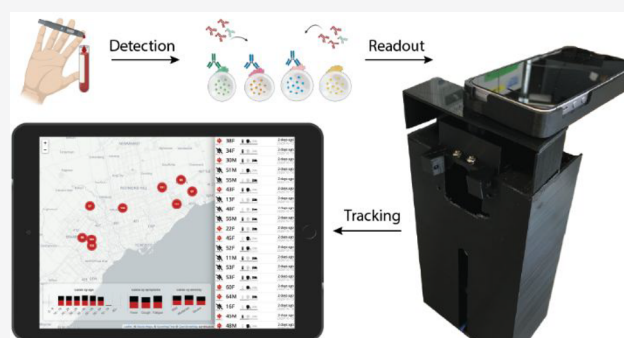
Article Recommendations



Supporting Information

**ABSTRACT:** The ability to rapidly diagnose, track, and disseminate information for SARS-CoV-2 is critical to minimize its spread. Here, we engineered a portable smartphone-based quantum barcode serological assay device for real-time surveillance of patients infected with SARS-CoV-2. Our device achieved a clinical sensitivity of 90% and specificity of 100% for SARS-CoV-2, as compared to 34% and 100%, respectively, for lateral flow assays in a head-to-head comparison. The lateral flow assay misdiagnosed ~2 out of 3 SARS-CoV-2 positive patients. Our quantum dot barcode device has ~3 times greater clinical sensitivity because it is ~140 times more analytically sensitive than lateral flow assays. Our device can diagnose SARS-CoV-2 at different sampling dates and infectious severity. We developed a databasing app to provide instantaneous results to inform patients, physicians, and public health agencies. This assay and device enable real-time surveillance of SARS-CoV-2 seroprevalence and potential immunity.

**KEYWORDS:** serological testing, smartphone diagnostics, SARS-CoV-2, COVID-19, real-time monitoring, quantum dot barcodes, immunoassay, multiplexing, database



## INTRODUCTION

SARS-CoV-2 has infected over 124 million people, causing over 2.7 million deaths globally as of March 24, 2021.<sup>1</sup> The accurate diagnosis of patients is crucial for treatment decisions and surveillance.<sup>2,3</sup> However, most diagnostic tools require centralized testing laboratories, trained personnel, and the manual entry of results.<sup>4</sup> These often lead to slow turnaround times and add stress to an overburdened healthcare system. Decentralized diagnostic tools from hospitals that are integrated with data reporting apps could potentially solve these issues.<sup>5</sup> Self-performed and automated central reporting of results could distribute testing loads, reduce delays, and enhance public health surveillance.

Smartphones have been explored for the development of portable and integrated diagnostics. They are equipped with high-resolution cameras, processing power, and connectivity and have high adoption rates in developing areas of the world.<sup>6–8</sup> These features make smartphone-based devices ideal for developing diagnostics that can be performed outside of hospitals. Nucleic acid testing, the current gold standard for detecting SARS-CoV-2, can integrate with smartphone-based devices. However, nucleic acid tests require extraction, transcription, amplification, and detection of the genome, making their full integration into one system a challenge. Both Ganguli et al. and Rodriguez-Manzano et al. demonstrated a

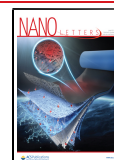
smartphone-based imaging system for SARS-CoV-2 nucleic acid diagnostics with amplification and detection but not extraction capability.<sup>9,10</sup> These tests will require RNA to be extracted before loading to the device. Nucleic acid tests are currently performed in the initial stage of infection. These tests may miss asymptomatic patients and cases because they must be administered in centralized facilities.

Integrating serological tests with smartphones would improve the diagnostic process because these tests have fewer labor-intensive steps in the workflow than nucleic acid tests for surveillance. Serological tests are easier to adapt for home or point-of-care use because samples are simpler to obtain (i.e., finger prick vs nasopharyngeal swab), and there is no need for extraction, heating, or amplification steps.<sup>11,12</sup> Serological diagnostics measure host antibodies that remain in circulation postinfection rather than directly detecting viral material present during infection.<sup>13,14</sup> As a result, they are the

**Received:** March 29, 2021

**Revised:** May 26, 2021

**Published:** June 10, 2021



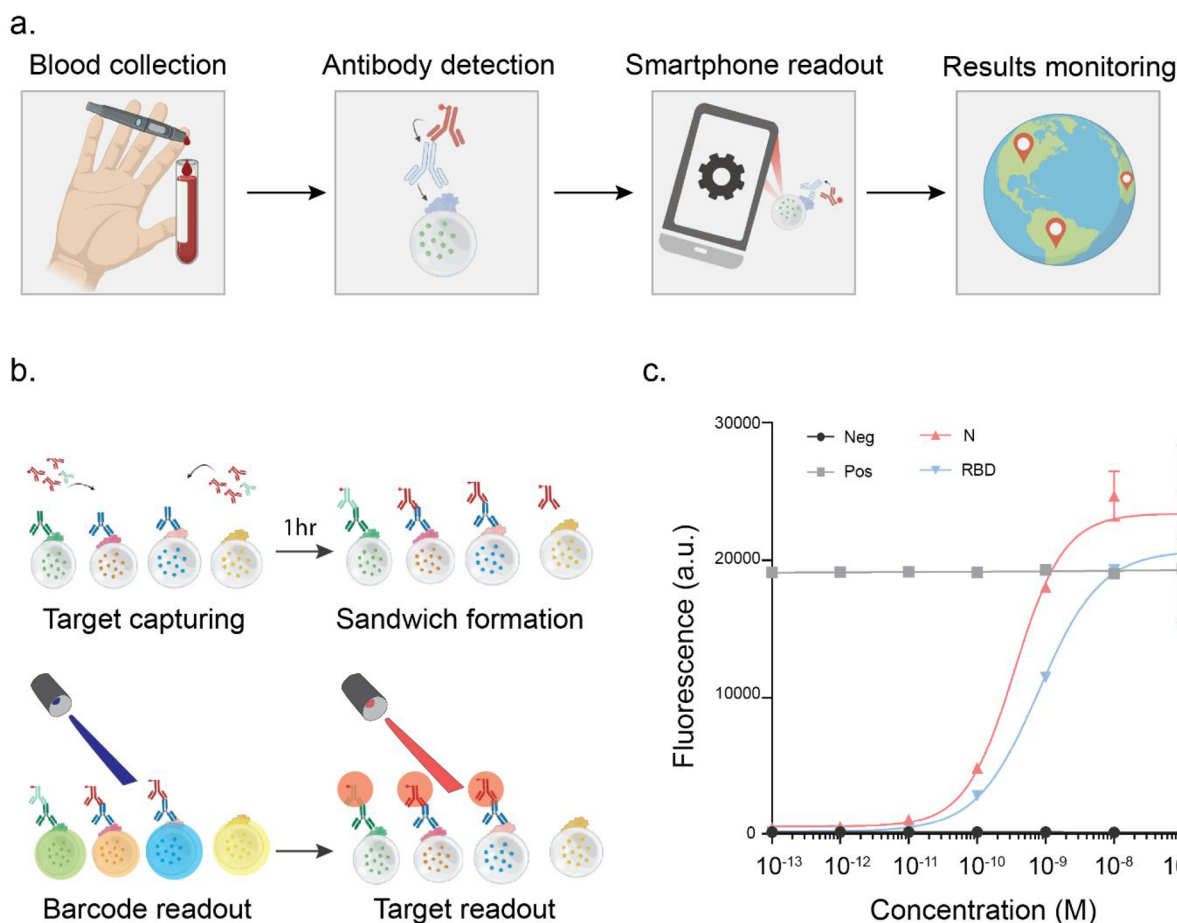


**Figure 1.** Quantum dot barcode (QDB) immunoassay for COVID-19 serological diagnostics. (a) Schematic for the smartphone antibody detection workflow. Patient serum samples are collected and incubated with QDBs to carry out the immunoassay. The assay results are read on a smartphone imaging device and uploaded to a real-time dashboard for monitoring. (b) Schematic for visualizing the QDB immunoassay workflow. The target antibody is first captured onto the antigen-coated QDBs. The fluorophore-conjugated secondary antibody then forms a sandwich structure with the target antibody. The laser excites the quantum dots and the fluorophore to identify the beads and the amount of target antibody. (c) Dose–response curve of a 4-plex assay including spike protein RBD (red), nucleocapsid protein (blue), a positive (gray), and negative control (black) ( $n = 3$  repeated tests; error bars: SD). Created with BioRender.com.

only tools capable of monitoring immune responses<sup>15</sup> and can estimate the total case count as they can retrospectively identify untested or asymptomatic cases or those associated with false-negative PCR results.<sup>16–18</sup> Most serology tests, such as enzyme-linked immunosorbent and chemiluminescent immunoassays (ELISA, CLIA), are only available through healthcare or reference centers owing to the equipment and trained laboratory personnel required for performing the assay. The only serological tools that are currently deployed at point-of-care are paper-based lateral flow assays. Their poor sensitivity and inconsistent performance have resulted in high rates of misclassification of cases.<sup>19</sup> There is a need to develop home-based serology tests for SARS-CoV-2 with the diagnostic performance of ELISA.

Here, we designed and built a smartphone-based diagnostic platform that automates the detection and reporting of SARS-CoV-2 serology testing. Our platform houses a smartphone imaging stage that automates quantitative readout of our assay, termed the *quantum dot barcode immunoassay*, and interfaces with a data dashboard that was built in-house (Figure 1a). We evaluated our imaging platform and demonstrated real-time reporting of the test results using a database and a dashboard.

## RESULTS AND DISCUSSION

Our strategy involves (a) quantum dot microbeads to capture target antibodies in serum, (b) a hand-held device to excite and image the microbead fluorescence, and (c) an app that relays the results to a centralized facility. We selected quantum dots for coding microbeads over fluorescent dye molecules because the quantum dot's continuous absorption profile, photostability, brightness, and narrow fluorescence emission simplify the instrumentation and software design needed for microbead identification and signal detection. These quantum dot properties also enable the engineering of a portable readout system. The microbeads are conjugated with viral proteins to capture antibodies in serum. Antibodies captured on the bead surface are bound by a complementary secondary probe labeled with a fluorophore that produces a different signal than the barcoded beads, forming a sandwich structure (Figure 1b). Different color quantum dot barcoded microbeads can be designed to detect different antibody targets (e.g., the detection of 4 targets involves 4 uniquely barcoded beads). A panel of multiple quantum dot barcoded microbeads can be simultaneously added to biological fluids for detection (Figure S1). We developed our smartphone reader to differentiate barcoded microbeads and secondary probe signals for

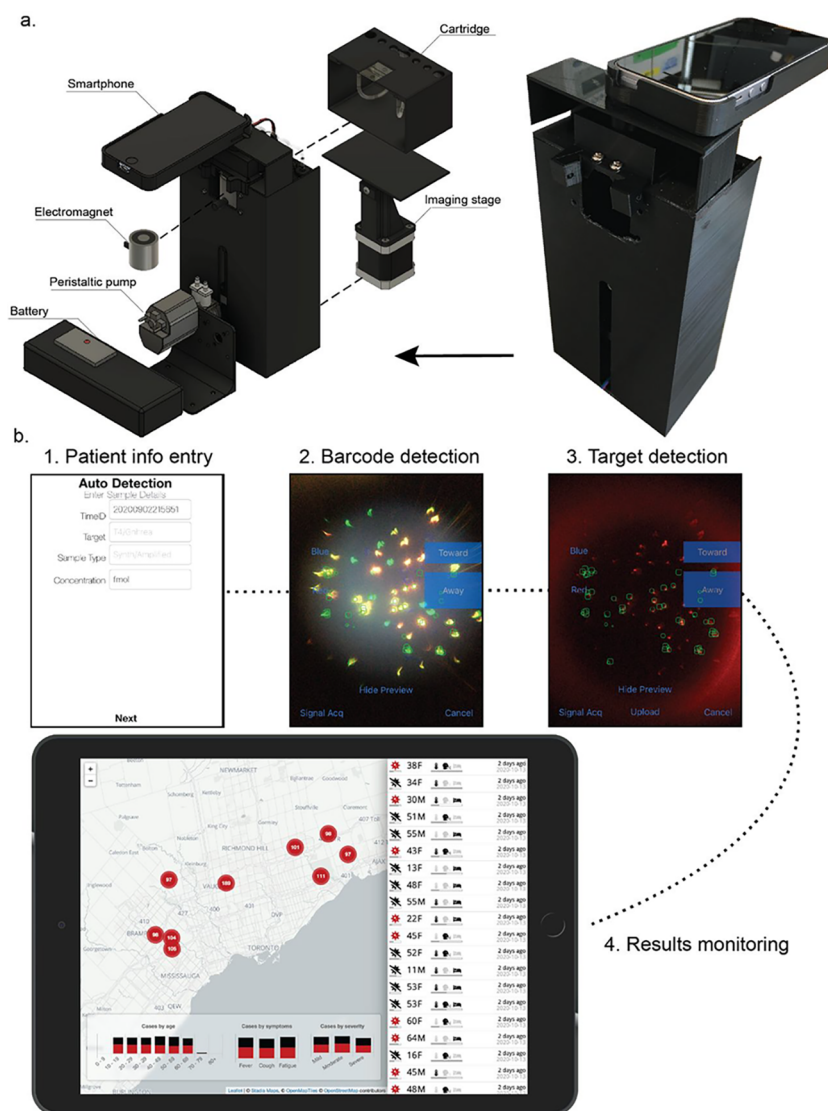


**Figure 2.** Smartphone imaging device for quantum dot barcode immunoassay. (a) Schematic for the smartphone imaging device. Right: picture of the device coupled to an iPhone SE. Left: breakdown of each device component. (b) Smartphone detection workflow. The smartphone app controls the imaging device and facilitates the assay readout. The results are uploaded to a database which can be displayed on a dashboard for real-time monitoring. Our written code for tracking can be accessed here: <https://github.com/BaderLab/covid19-dashboard>.

multiplexed (multiple targets) readout. These results are uploaded to a database for real-time monitoring.

**Quantum Dot Barcode Assay.** First, we engineered and tested a panel of quantum dot barcodes for SARS-CoV-2 serology tests. Our multiplex panel includes four barcodes: two barcodes for different antibodies against the virus and a positive and negative internal control (Figure 1). Assays that detect multiple antibodies rather than a single target have increased sensitivities and specificities, provide more information per run, and improve detection of rapidly mutating pathogens. The two anti-SARS-CoV-2 antibodies selected were anti-S1 receptor-binding domain immunoglobulin G (anti-RBD) and anti-nucleocapsid IgG (anti-N). Anti-RBD is highly specific for SARS-CoV-2 and correlates with neutralizing antibodies.<sup>20,21</sup> Anti-N IgG is abundant in infected patients.<sup>22</sup> IgG was chosen as a target instead of IgM or IgA because IgG emerges in the body in the early stages of infection and circulates for up to 10 months or longer. IgM and IgA emerge earlier but are less consistent than IgG in serological testing.<sup>23</sup>

We synthesized four spectrally different barcoded quantum dot microbeads with iron oxide nanoparticles through a concentration-controlled flow-focusing method (Figure S2, Methods).<sup>24</sup> The unique spectral properties of each barcode are created by combining different quantum dot concentrations and emission wavelengths (Figure S3). Each optically distinct bead was conjugated with SARS-CoV-2 nucleocapsid (N) antigens, SARS-CoV-2 S1 RBD (RBD) antigens, positive (pos) control, or negative (neg) control proteins using carbodiimide chemistry (Figure S4). First, we used flow cytometry to determine the dynamic range and limits of detection (LoD) of our assay (Figures S5 and S6). These experiments confirmed that microbead-coated antigens can recognize the targets and are unaffected by the reaction conditions. Our multiplex barcode assay reported an LoD of 1.99 and 0.11 pM for the nucleocapsid-coated and S1-RBD-coated microbeads, respectively (Figure 1c). Performing the assay in serum versus buffer solution had no significant difference in the LoD of both barcodes (Figure S7). A minor decrease in LoD was observed in whole blood compared to

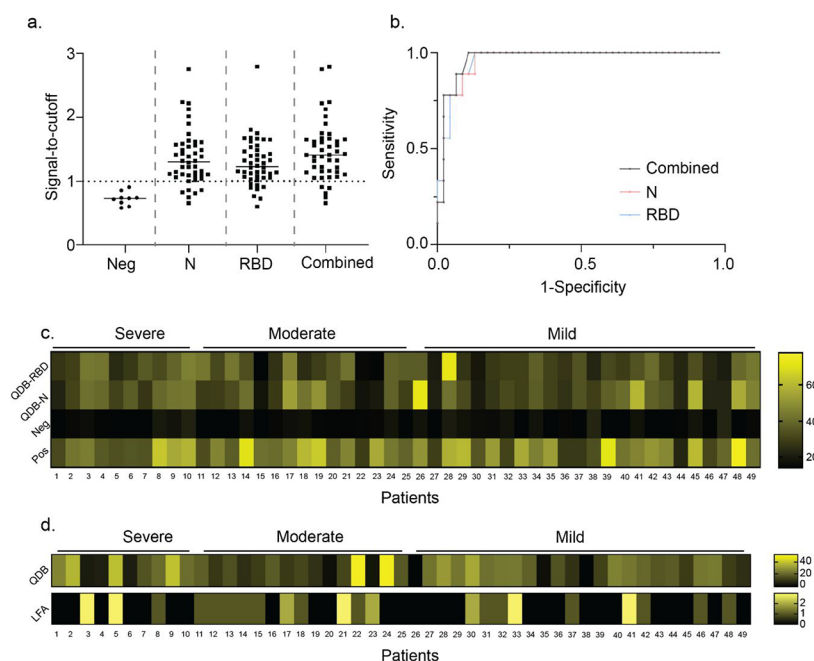


**Figure 3.** Clinical performance evaluation of the smartphone quantum dot device. (a) Forty-nine positive convalescent patient serum samples were assayed and read on the smartphone imaging device. (b) Receiver operating characteristic curves for the assay. (c) Two different QDB-RBD and QDB-N detection signals via smartphone imaging from the different patient samples are shown as a heatmap. We also include the result for the positive (pos) and negative control (neg) QDB. Only one of the two biomarkers must be successfully detected to determine a positive result. The legend indicates the corresponding color for the absolute fluorescence intensity. (d) QDB signal here represents the highest signal from either the RBD or N. A comparison of the results with lateral flow assay shows that the QDB assay/smartphone reader has better performance. Of note, for quantum dot device readouts, each cell represents the fluorescent readout for the corresponding barcodes. For lateral flow assay, each cell represents a user input value between 1 and 3 to indicate the band visibility (0 being negative). The patient samples are grouped based on disease severity.

serum (Figure S8). We found minimal cross-reactivity between each of our microbead sets (Figure S9). We benchmarked the performance of our multiplexed assay to a highly sensitive commercial anti-RBD IgG enzyme-linked immunoassay (ELISA, Euroimmun) selected from a list of prevalidated ELISA products.<sup>25</sup> The ELISA detected the anti-RBD IgG (same clone) used in our QDB assay at an LoD of 2.1 pM (Figure S10), which is comparable to the LoD of the QDB assay. We also conducted a small pilot study using patient samples to ensure the biological matrix did not interfere with the assay. Our pilot study showed that our microbead assay performed similarly to ELISA for diagnosing serological biomarkers (Figures S11 and S12). The purpose of these experiments was to benchmark our assay's performance to the serological test gold standard ELISA.

**Smartphone Imaging Platform.** We engineered a smartphone device for assay readout and communicating results. It consists of four main components: (1) a microfluidic system for mixing, washing, and isolating of microbeads, (2) an optical train with an imaging stage to excite, collect, and focus appropriate wavelengths of light, (3) a smartphone equipped with an application that automates the classification of barcoded microbeads, and (4) a database and dashboard where assay results can be uploaded and displayed. All the components were held together in a 3-D printed case (Figure 2a). The smartphone is attached to an adapter on the top of the imaging system, which can be modulated to the model of the smartphone being used.

Once the barcode assay is complete, the beads are injected into the imaging stage, where the bead is flowed into the camera view and magnetically immobilized to enable

excitation. The barcodes are excited by a single laser, and their signals are collected by the smartphone. Once the barcode signal has been captured, a switch operates a change in the laser and filter for the acquisition of signal from the secondary probe. The microbead and the secondary probe signals are overlaid and automatically transferred to a database for analysis. The optical signal from the microbead identifies the target serological biomarker. If the secondary probe signal is overlaid, it will indicate a positive detection for that specific protein biomarker. The signal intensity determines the concentration of proteins in serum. Lastly, the results and geographical information are transferred from our database to a dashboard for real-time monitoring of test results (Figure 2b; full code is available in the Supporting Information). The dashboard is designed to update results instantaneously upon assay completion. The dashboard provides information on patient age, gender, and severity and can relay data to patients, physicians, and public health units. In the dashboard, the central view is a map with the geographical information captured by the smartphone to locate each case. As the map is zoomed in and out, cases are shown in clusters according to the zoom level. The side panel shows a real-time feed of each test visible within the map viewport (sorted by date). Selecting a test will provide more details about that individual case. Histogram charts are available along the bottom, showing a number of cases over time, and delineated by age, symptoms, and severity. Our dashboard is also optimized for various screen sizes and with full support for mobile devices.

We characterized the analytical limit of detection of the smartphone imaging system by performing a sandwich assay with synthetic anti-RBD IgG. The smartphone reader had an

LoD at 0.7 nM for detecting anti-RBD IgG (Figure S13). We used the same samples to characterize the performance of a conventional lateral flow assay detecting anti-N IgG and found it had a limit of detection of 100 nM (Figure S14). The analytical performance of our assay is at least 140-fold higher than that of the lateral flow assay.

**Clinical Performance Evaluation.** We evaluated the clinical performance of our quantum dot microbead assay/smartphone device and compared it to a lateral flow assay. We obtained 50 samples from patients that were previously confirmed for COVID-19 by RT-PCR and confirmed as seropositive by an in-house ELISA<sup>26</sup> that detects both anti-N and anti-S1 antibodies. One sample was not used because the sample volume was too low for analysis. Our assay reported a sensitivity of 84% (95% CI: 70–92%) and 88% (95% CI: 77–96%) for anti-RBD IgG and anti-nucleocapsid IgG, respectively. The specificity of both antibody types was 100% (95% CI: 46–100%) (Figure 3a). The overall assay sensitivity can be improved to 90% (95% CI: 77–96%) while maintaining 100% specificity (95% CI: 46–100%) using a multiplexed analysis (Figure 3b). In our multiplex analysis, we classify a sample as positive if one or both antibody types are detected. Patients reporting positive for one type of IgG but not the other could result from some patients having increased levels of one type of IgG over the other.

We compared the clinical performance of our smartphone device to a point-of-care lateral flow immunoassay. Lateral flow assays are currently the only marketed point-of-care serological detection method but have low sensitivities resulting in faint test lines that users often incorrectly interpret. The samples used with the lateral flow assay were the same as the ones used with the smartphone reader. We report a sensitivity and specificity of 34% (95% CI: 22–50%) and 100% (95% CI: 46–100%) using the lateral flow assay, respectively.

Furthermore, we evaluated the performance of our device across a range of antibody titers. It has been reported that asymptomatic and less severe cases are associated with lower antibody titers.<sup>27,28</sup> The patient samples ranged in their disease severity and included intensive care unit inpatients with severe illness (ICU), non-ICU inpatients with moderate illness, and outpatients with mild illness. We delineated our diagnostic results to explore the effect of disease severity on our assay across the collected patient samples. We grouped results from our assay based on patient disease severity (Figure 3c,d) and found minimal variation. On the contrary, the lateral flow assay misdiagnosed patients at varying disease severities, especially the mild symptom cases, when compared to our assay (as indicated by the higher number of black bars in the Figure 3d heatmap). Our assay system could detect antibodies in symptomatic patients with a range of disease severities, while lateral flow assay has significantly poorer clinical performance.

We assessed whether our diagnostic could be used to track SARS-CoV-2 immune responses over time. Although the link between the production of antibodies and COVID-19 immunity is not yet clear, serological tests may be useful for evaluating immune responses generated after vaccination to monitor levels of immunity over time in patients.<sup>29</sup> We delineated the patients based on the number of days after symptom onset (Figure 4a). The data presented show the successful detection of SARS-CoV-2 patients over 104 days using our quantum dot assay/smartphone device as compared to the lateral flow assay (Figure 4b). The lateral flow assay misdiagnosed patients over the range of dates and was

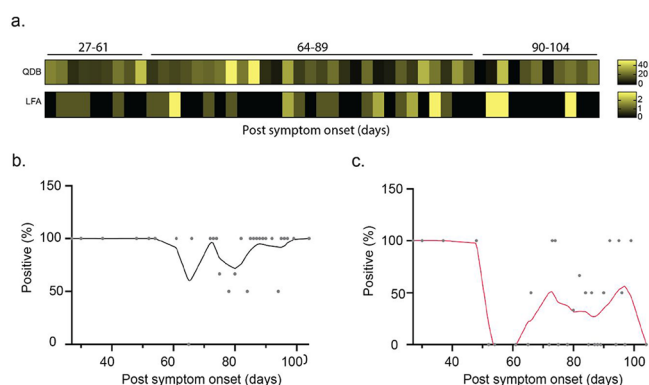


**Figure 4.** Tracking of potential disease severity and immunity using our smartphone quantum dot device. (a) Each patient's assay readout for both the smartphone quantum dot device and lateral flow assay based on collection date. The numbers above the heatmap indicate the number of days since the patients developed symptoms at the time of sampling. For quantum dot device readouts, each cell represents the fluorescent readout for the corresponding barcodes. For lateral flow assay, each cell represents a user input value between 1 and 3 to indicate how visible the band is (0 being negative). (b) Quantum dot barcode results: percent positive detection based on collection date. The positivity rate indicates what percentage of samples identified as positive at any given day. (c) Lateral flow assay: percent positive detection based on collection date. The positivity rate indicates the percentage of samples positively identified at any given day.

unreliable after day 54 with sensitivities below 50% (Figure 4c). Our assay maintained high sensitivity across the sample data range. Our device can detect levels of antibodies as they decrease over time, but the lateral flow assay cannot.

Of note, clinical samples often exhibit a wide range of target molecule concentration. Antibody response for SARS-CoV-2 has been found to be dependent on age,<sup>30</sup> sex,<sup>31</sup> comorbidity,<sup>32</sup> and severity.<sup>33</sup> It is therefore important for the diagnostic assay to be as accurate as possible to account for the variability in clinical samples.

Lateral flow immunoassays are currently the gold standard method in portable point-of-care devices. Our results clearly show these assays do not have the sensitivity for the long-term tracking of SARS-CoV-2. Lateral flow immunoassays may have difficulty in identifying seroprevalence in different populations and the response to COVID-19 vaccines. As COVID-19 vaccine programs are implemented, serological testing will be needed in order to validate their effectiveness and to monitor patient immune status over time.<sup>34,35</sup> Developing a reliable point-of-care serological test could enable home testing or in family doctor offices. Our assay has the advantage of ELISA-like analytical sensitivities but is portable and can be used at point-of-care. All reagents can be placed in a tablet for easy transport and utility.<sup>36</sup>

Diagnostic assays are only one of the key parameters in the diagnostic framework for managing the COVID-19 pandemic. A second key parameter is the ability to rapidly relay test results to databases for use by the general public, clinicians, and public health agencies. The need for rapid communication of information has led many countries to start developing smartphone apps to monitor results in real-time.<sup>37</sup> The data in the app are manually inputted by individuals typically diagnosed with molecular tests or linked to public health laboratories creating a lag between diagnosis and information

reporting. Our quantum dot assay/smartphone system allows for a quicker strategy to detect, input, and relay test results to key stakeholders. Real-time access to diagnostic information enables the public and health agencies to be informed of the pandemic's extent, take precautions, and implement public health measures to minimize transmission. Our overall workflow and concept can be adapted to SARS-CoV-2 genetic tests once a point-of-care test is developed.

The next step is to automate the liquid handling and assay readout. This automation process involves the optimization of engineering parameters and will be conducted in the productization stage of technology development. Another research direction is to develop a serological test for monitoring SARS-CoV-2 variants. This requires the development of antibodies against SARS-CoV-2 variants. Once available, the quantum dot barcode panels could include different variants to enable multiplex analysis. It would be interesting to evaluate the impact of the mutation on assay performance of serological tests.

The limitations of our diagnostic technology relate to patient data storage and security. Although real-time access to diagnostic results is a faster communication method, it is important to store patient data securely. Currently, we use Google Firebase to host cloud data storage. In the future, our system and others would need to consider the use of decentralized databases that comply with the necessary privacy laws to ensure assay results and patient data are securely stored and transmitted.

## CONCLUSION

The broader concept of incorporating smartphones with diagnostic testing could rapidly present test results allowing policymakers to monitor pandemics in real-time. Our smartphone imaging platform and reporting app can be adapted to different smartphones by changing the holder design. While lateral flow tests can be adapted with smartphones, their low sensitivity results in too many false negatives to be an effective surveillance tool. We envision that our device will be crucial for monitoring vaccine effectiveness and the requirement for more studies on immunity. Our device may allow local doctors' clinics to evaluate patients at prevaccination, monitor potential immunity postvaccination, and rapidly surveil and track the seroprevalence of COVID-19 in the population. Our platform has the potential to be used for antibody detection, immunity surveillance, and vaccination-induced seroconversion monitoring—all of which is crucial for the healthcare system to control and combat the current COVID-19 pandemic.

## ASSOCIATED CONTENT

### Supporting Information

The Supporting Information is available free of charge at <https://pubs.acs.org/doi/10.1021/acs.nanolett.1c01280>.

Assay schematics, quantum dot barcode characterization, assay optimization, cross-reactivity assessment, analytical and clinical assay validations, assay benchmarks, materials, and methods (PDF)

## AUTHOR INFORMATION

### Corresponding Author

Warren C. W. Chan – Department of Chemistry, University of Toronto, Toronto, Ontario M5S 3H6, Canada; Institute of

Biomedical Engineering, University of Toronto, Toronto, Ontario M5S 3G9, Canada; Terrence Donnelly Centre for Cellular and Biomolecular Research, University of Toronto, Toronto, Ontario M5S 3E1, Canada; Department of Chemical Engineering, University of Toronto, Toronto, Ontario M5S 3E5, Canada; Department of Materials Science and Engineering, University of Toronto, Toronto, Ontario M5S 3E1, Canada; [orcid.org/0000-0001-5435-4785](https://orcid.org/0000-0001-5435-4785); Email: [warren.chan@utoronto.ca](mailto:warren.chan@utoronto.ca)

## Authors

**Yuwei Zhang** – Department of Chemistry, University of Toronto, Toronto, Ontario M5S 3H6, Canada; Terrence Donnelly Centre for Cellular and Biomolecular Research, University of Toronto, Toronto, Ontario M5S 3E1, Canada

**Ayden Malekjahani** – Institute of Biomedical Engineering, University of Toronto, Toronto, Ontario M5S 3G9, Canada; Terrence Donnelly Centre for Cellular and Biomolecular Research, University of Toronto, Toronto, Ontario M5S 3E1, Canada

**Buddhisha N. Udugama** – Institute of Biomedical Engineering, University of Toronto, Toronto, Ontario M5S 3G9, Canada; Terrence Donnelly Centre for Cellular and Biomolecular Research, University of Toronto, Toronto, Ontario M5S 3E1, Canada

**Pranav Kadhiresan** – Institute of Biomedical Engineering, University of Toronto, Toronto, Ontario M5S 3G9, Canada; Terrence Donnelly Centre for Cellular and Biomolecular Research, University of Toronto, Toronto, Ontario M5S 3E1, Canada

**Hongmin Chen** – Institute of Biomedical Engineering, University of Toronto, Toronto, Ontario M5S 3G9, Canada; Terrence Donnelly Centre for Cellular and Biomolecular Research, University of Toronto, Toronto, Ontario M5S 3E1, Canada

**Matthew Osborne** – Institute of Biomedical Engineering, University of Toronto, Toronto, Ontario M5S 3G9, Canada; Terrence Donnelly Centre for Cellular and Biomolecular Research, University of Toronto, Toronto, Ontario M5S 3E1, Canada

**Max Franz** – Terrence Donnelly Centre for Cellular and Biomolecular Research, University of Toronto, Toronto, Ontario M5S 3E1, Canada

**Mike Kucera** – Terrence Donnelly Centre for Cellular and Biomolecular Research, University of Toronto, Toronto, Ontario M5S 3E1, Canada

**Simon Plenderleith** – Biological Sciences, Sunnybrook Research Institute, Toronto, Ontario M4N 3M5, Canada

**Lily Yip** – Biological Sciences, Sunnybrook Research Institute, Toronto, Ontario M4N 3M5, Canada; [orcid.org/0000-0002-7387-0387](https://orcid.org/0000-0002-7387-0387)

**Gary D. Bader** – Terrence Donnelly Centre for Cellular and Biomolecular Research, University of Toronto, Toronto, Ontario M5S 3E1, Canada; Department of Molecular Genetics, University of Toronto, Toronto, Ontario M5G 1A8, Canada; Department of Computer Science, University of Toronto, Toronto, Ontario M5S 2E4, Canada; Lunenfeld-Tanenbaum Research Institute, Mount Sinai Hospital, Sinai Health System, Toronto, Ontario M5G 1X5, Canada; Princess Margaret Cancer Centre, University Health Network, Toronto, Ontario M5G 2C1, Canada

**Vanessa Tran** – Public Health Ontario, Toronto, Ontario M5G 1M1, Canada; Department of Laboratory Medicine

and Pathobiology, Faculty of Medicine, University of Toronto, Toronto, Ontario M5S 1A8, Canada

**Jonathan B. Gubbay** – Public Health Ontario, Toronto, Ontario M5G 1M1, Canada; Department of Laboratory Medicine and Pathobiology, Faculty of Medicine, University of Toronto, Toronto, Ontario M5S 1A8, Canada

**Allison McGeer** – Lunenfeld-Tanenbaum Research Institute and Department of Microbiology, Mount Sinai Hospital, Sinai Health System, Toronto, Ontario M5G 1X5, Canada; Dalla Lana School of Public Health, University of Toronto, Toronto, Ontario M5T 3M7, Canada

**Samira Mubareka** – Department of Laboratory Medicine and Pathobiology, Faculty of Medicine, University of Toronto, Toronto, Ontario M5S 1A8, Canada; Biological Sciences, Sunnybrook Research Institute, Toronto, Ontario M4N 3M5, Canada

Complete contact information is available at:

<https://pubs.acs.org/10.1021/acs.nanolett.1c01280>

### Author Contributions

□ Y.Z. and A.M. contributed equally to this work.

### Notes

The authors declare the following competing financial interest(s): W.C.W.C. co-founded start-up company LunaNanotech.

### ACKNOWLEDGMENTS

We acknowledge the Canadian Institute of Health Research (CIHR, FDN-159932; MOP-130143), Canadian Research Chairs program (950-223824), Collaborative Health Research Program (CPG-158270-S and CHRPS23436-18-S), and Connaught ISI (313897) for funding support. Y.Z. thanks the Ontario Ministry of Training, Colleges and Universities and the University of Toronto for the Ontario Graduate Scholarship. A.M. thanks the Canada Graduate Scholarship (NSERC) and the NRC-CRAFT fellowship. We thank H. Kozlowski for help with experimental ideation and manuscript editing.

### REFERENCES

- (1) COVID-19 Map, Johns Hopkins Coronavirus Resource Center <https://coronavirus.jhu.edu/map.html> (accessed December 1, 2020).
- (2) Weissleder, R.; Lee, H.; Ko, J.; Pittet, M. J. COVID-19 Diagnostics in Context. *Sci. Transl. Med.* **2020**, *12* (546), eabc1931.
- (3) Udugama, B.; Kadhiresan, P.; Kozlowski, H. N.; Malekjahani, A.; Osborne, M.; Li, V. Y. C.; Chen, H.; Mubareka, S.; Gubbay, J. B.; Chan, W. C. W. Diagnosing COVID-19: The Disease and Tools for Detection. *ACS Nano* **2020**, *14* (4), 3822–3835.
- (4) Nguyen, T.; Duong Bang, D.; Wolff, A. 2019 Novel Coronavirus Disease (COVID-19): Paving the Road for Rapid Detection and Point-of-Care Diagnostics. *Micromachines* **2020**, *11* (3), 306.
- (5) Brendish, N. J.; Poole, S.; Naidu, V. V.; Mansbridge, C. T.; Norton, N. J.; Wheeler, H.; Presland, L.; Kidd, S.; Cortes, N. J.; Borca, F.; Phan, H.; Babbage, G.; Visseaux, B.; Ewings, S.; Clark, T. W. Clinical Impact of Molecular Point-of-Care Testing for Suspected COVID-19 in Hospital (COV-19POC): A Prospective, Interventional, Non-Randomised, Controlled Study. *Lancet Respir. Med.* **2020**, *8*, 1192–1200.
- (6) Wood, C. S.; Thomas, M. R.; Budd, J.; Mashamba-Thompson, T. P.; Herbst, K.; Pillay, D.; Peeling, R. W.; Johnson, A. M.; McKendry, R. A.; Stevens, M. M. Taking Connected Mobile-Health Diagnostics of Infectious Diseases to the Field. *Nature* **2019**, *566*, 467–474.

(7) Malekjahani, A.; Sindhvani, S.; Syed, A. M.; Chan, W. C. W. Engineering Steps for Mobile Point-of-Care Diagnostic Devices. *Acc. Chem. Res.* **2019**, *52* (9), 2406–2414.

(8) Nayak, S.; Blumenfeld, N. R.; Laksanasopin, T.; Sia, S. K. Point-of-Care Diagnostics: Recent Developments in a Connected Age. *Anal. Chem.* **2017**, *89* (1), 102–123.

(9) Ganguli, A.; Mostafa, A.; Berger, J.; Aydin, M. Y.; Sun, F.; Ramirez, S. A. S. de; Valera, E.; Cunningham, B. T.; King, W. P.; Bashir, R. Rapid Isothermal Amplification and Portable Detection System for SARS-CoV-2. *Proc. Natl. Acad. Sci. U. S. A.* **2020**, *117* (37), 22727–22735.

(10) Rodriguez-Manzano, J.; Malpartida-Cardenas, K.; Moser, N.; Pennisi, I.; Cavuto, M.; Miglietta, L.; Moniri, A.; Penn, R.; Satta, G.; Randell, P.; Davies, F.; Bolt, F.; Barclay, W.; Holmes, A.; Georgiou, P. Handheld Point-of-Care System for Rapid Detection of SARS-CoV-2 Extracted RNA in under 20 min. *ACS Cent. Sci.* **2021**, *7* (2), 307–317.

(11) Valentine-Graves, M.; Hall, E.; Guest, J. L.; Adam, E.; Valencia, R.; Shinn, K.; Hardee, I.; Sanchez, T.; Siegler, A. J.; Sullivan, P. S. At-Home Self-Collection of Saliva, Oropharyngeal Swabs and Dried Blood Spots for SARS-CoV-2 Diagnosis and Serology: Post-Collection Acceptability of Specimen Collection Process and Patient Confidence in Specimens. *PLoS One* **2020**, *15*, e0236775.

(12) Pokhrel, P.; Hu, C.; Mao, H. Detecting the Coronavirus (COVID-19). *ACS Sens.* **2020**, *5*, 2283–2296.

(13) Peeling, R. W.; Wedderburn, C. J.; Garcia, P. J.; Boeras, D.; Fongwen, N.; Nkengasong, J.; Sall, A.; Tanuri, A.; Heymann, D. L. Serology Testing in the COVID-19 Pandemic Response. *Lancet Infect. Dis.* **2020**, *20*, e245–e249.

(14) To, K. K.-W.; Tsang, O. T.-Y.; Leung, W.-S.; Tam, A. R.; Wu, T.-C.; Lung, D. C.; Yip, C. C.-Y.; Cai, J.-P.; Chan, J. M.-C.; Chik, T. S.-H.; Lau, D. P.-L.; Choi, C. Y.-C.; Chen, L.-L.; Chan, W.-M.; Chan, K.-H.; Ip, J. D.; Ng, A. C.-K.; Poon, R. W.-S.; Luo, C.-T.; Cheng, V. C.-C.; Chan, J. F.-W.; Hung, I. F.-N.; Chen, Z.; Chen, H.; Yuen, K.-Y. Temporal Profiles of Viral Load in Posterior Oropharyngeal Saliva Samples and Serum Antibody Responses during Infection by SARS-CoV-2: An Observational Cohort Study. *Lancet Infect. Dis.* **2020**, *20*, 565–574.

(15) Ni, L.; Ye, F.; Cheng, M.-L.; Feng, Y.; Deng, Y.-Q.; Zhao, H.; Wei, P.; Ge, J.; Gou, M.; Li, X.; Sun, L.; Cao, T.; Wang, P.; Zhou, C.; Zhang, R.; Liang, P.; Guo, H.; Wang, X.; Qin, C.-F.; Chen, F.; Dong, C. Detection of SARS-CoV-2-Specific Humoral and Cellular Immunity in COVID-19 Convalescent Individuals. *Immunity* **2020**, *52* (6), 971–977.

(16) Sethuraman, N.; Jeremiah, S. S.; Ryo, A. Interpreting Diagnostic Tests for SARS-CoV-2. *JAMA* **2020**, *323* (22), 2249–2251.

(17) Long, Q.-X.; Liu, B.-Z.; Deng, H.-J.; Wu, G.-C.; Deng, K.; Chen, Y.-K.; Liao, P.; Qiu, J.-F.; Lin, Y.; Cai, X.-F.; Wang, D.-Q.; Hu, Y.; Ren, J.-H.; Tang, N.; Xu, Y.-Y.; Yu, L.-H.; Mo, Z.; Gong, F.; Zhang, X.-L.; Tian, W.-G.; Hu, L.; Zhang, X.-X.; Xiang, J.-L.; Du, H.-X.; Liu, H.-W.; Lang, C.-H.; Luo, X.-H.; Wu, S.-B.; Cui, X.-P.; Zhou, Z.; Zhu, M.-M.; Wang, J.; Xue, C.-J.; Li, X.-F.; Wang, L.; Li, Z.-J.; Wang, K.; Niu, C.-C.; Yang, Q.-J.; Tang, X.-J.; Zhang, Y.; Liu, X.-M.; Li, J.-J.; Zhang, D.-C.; Zhang, F.; Liu, P.; Yuan, J.; Li, Q.; Hu, J.-L.; Chen, J.; Huang, A.-L. Antibody Responses to SARS-CoV-2 in Patients with COVID-19. *Nat. Med.* **2020**, *26* (6), 845–848.

(18) Ripperger, T. J.; Uhrlaub, J. L.; Watanabe, M.; Wong, R.; Castaneda, Y.; Pizzato, H. A.; Thompson, M. R.; Bradshaw, C.; Weinkauff, C. C.; Bime, C.; Erickson, H. L.; Knox, K.; Bixby, B.; Parthasarathy, S.; Chaudhary, S.; Natt, B.; Cristan, E.; El Aini, T.; Rischard, F.; Campion, J.; Chopra, M.; Insel, M.; Sam, A.; Knepler, J. L.; Capaldi, A. P.; Spier, C. M.; Dake, M. D.; Edwards, T.; Kaplan, M. E.; Scott, S. J.; Hypes, C.; Mosier, J.; Harris, D. T.; LaFleur, B. J.; Sprissler, R.; Nikolich-Zugich, J.; Bhattacharya, D. Orthogonal SARS-CoV-2 Serological Assays Enable Surveillance of Low-Prevalence Communities and Reveal Durable Humoral Immunity. *Immunity* **2020**, *53*, 925–933.

- (19) Lisboa Bastos, M.; Tavaziva, G.; Abidi, S. K.; Campbell, J. R.; Haraoui, L.-P.; Johnston, J. C.; Lan, Z.; Law, S.; MacLean, E.; Trajman, A.; Menzies, D.; Benedetti, A.; Ahmad Khan, F. Diagnostic Accuracy of Serological Tests for Covid-19: Systematic Review and Meta-Analysis. *BMJ.* **2020**, *370*, m2516.
- (20) Chen, X.; Pan, Z.; Yue, S.; Yu, F.; Zhang, J.; Yang, Y.; Li, R.; Liu, B.; Yang, X.; Gao, L.; Li, Z.; Lin, Y.; Huang, Q.; Xu, L.; Tang, J.; Hu, L.; Zhao, J.; Liu, P.; Zhang, G.; Chen, Y.; Deng, K.; Ye, L. Disease Severity Dictates SARS-CoV-2-Specific Neutralizing Antibody Responses in COVID-19. *Signal Transduct Target Ther* **2020**, *5*, 180.
- (21) Bošnjak, B.; Stein, S. C.; Willenzon, S.; Cordes, A. K.; Puppe, W.; Bernhardt, G.; Ravens, L.; Ritter, C.; Schultze-Florey, C. R.; Gödecke, N.; Martens, J.; Kleine-Weber, H.; Hoffmann, M.; Cossmann, A.; Yilmaz, M.; Pink, I.; Hoepfer, M. M.; Behrens, G. M. N.; Pöhlmann, S.; Blasczyk, R.; Schulz, T. F.; Förster, R. Low Serum Neutralizing Anti-SARS-CoV-2 S Antibody Levels in Mildly Affected COVID-19 Convalescent Patients Revealed by Two Different Detection Methods. *Cell. Mol. Immunol.* **2021**, *18*, 936–944.
- (22) Chen, Y.; Li, L. SARS-CoV-2: Virus Dynamics and Host Response. *Lancet Infect. Dis.* **2020**, *20* (5), 515–516.
- (23) Whitman, J. D.; Hiatt, J.; Mowery, C. T.; Shy, B. R.; Yu, R.; Yamamoto, T. N.; Rathore, U.; Goldgof, G. M.; Whitty, C.; Woo, J. M.; Gallman, A. E.; Miller, T. E.; Levine, A. G.; Nguyen, D. N.; Bapat, S. P.; Balcerek, J.; Bylsma, S. A.; Lyons, A. M.; Li, S.; Wong, A. W.-Y.; Gillis-Buck, E. M.; Steinhart, Z. B.; Lee, Y.; Apathy, R.; Lipke, M. J.; Smith, J. A.; Zheng, T.; Boothby, I. C.; Isaza, E.; Chan, J.; Acenas, D. D., 2nd; Lee, J.; Macrae, T. A.; Kyaw, T. S.; Wu, D.; Ng, D. L.; Gu, W.; York, V. A.; Eskandarian, H. A.; Callaway, P. C.; Warrior, L.; Moreno, M. E.; Levan, J.; Torres, L.; Farrington, L. A.; Loudermilk, R. P.; Koshal, K.; Zorn, K. C.; Garcia-Beltran, W. F.; Yang, D.; Astudillo, M. G.; Bernstein, B. E.; Gelfand, J. A.; Ryan, E. T.; Charles, R. C.; Iafate, A. J.; Lennerz, J. K.; Miller, S.; Chiu, C. Y.; Stramer, S. L.; Wilson, M. R.; Manglik, A.; Ye, C. J.; Krogan, N. J.; Anderson, M. S.; Cyster, J. G.; Ernst, J. D.; Wu, A. H. B.; Lynch, K. L.; Bern, C.; Hsu, P. D.; Marson, A. Evaluation of SARS-CoV-2 Serology Assays Reveals a Range of Test Performance. *Nat. Biotechnol.* **2020**, *38* (10), 1174–1183.
- (24) Fournier-Bidoz, S.; Jennings, T. L.; Klostranec, J. M.; Fung, W.; Rhee, A.; Li, D.; Chan, W. C. W. Facile and Rapid One-Step Mass Preparation of Quantum-Dot Barcodes. *Angew. Chem., Int. Ed.* **2008**, *47* (30), 5577–5581.
- (25) SARS-CoV-2 Diagnostic Pipeline; <https://www.finndx.org/covid-19/pipeline/> (accessed November 25, 2020).
- (26) Isho, B.; Abe, K. T.; Zuo, M.; Jamal, A. J.; Rathod, B.; Wang, J. H.; Li, Z.; Chao, G.; Rojas, O. L.; Bang, Y. M.; Pu, A.; Christie-Holmes, N.; Gervais, C.; Ceccarelli, D.; Samavarchi-Tehrani, P.; Guvenc, F.; Budylowski, P.; Li, A.; Paterson, A.; Yue, F. Y.; Marin, L. M.; Caldwell, L.; Wrana, J. L.; Colwill, K.; Sicheri, F.; Mubareka, S.; Gray-Owen, S. D.; Drews, S. J.; Siqueira, W. L.; Barrios-Rodiles, M.; Ostrowski, M.; Rini, J. M.; Durocher, Y.; McGeer, A. J.; Gommerman, J. L.; Gingras, A.-C. Persistence of Serum and Saliva Antibody Responses to SARS-CoV-2 Spike Antigens in COVID-19 Patients. *Sci. Immunol.* **2020**, *5* (52), eabe5511.
- (27) Kowitdamrong, E.; Puthanakit, T.; Jantarabenjakul, W.; Prompetchara, E.; Suchartlikitwong, P.; Pucharoen, O.; Hirankarn, N. Antibody Responses to SARS-CoV-2 in Patients with Differing Severities of Coronavirus Disease 2019. *PLoS One* **2020**, *15* (10), e0240502.
- (28) MGH COVID-19 Collection & Processing Team. Viral Epitope Profiling of COVID-19 Patients Reveals Cross-Reactivity and Correlates of Severity. *Science* **2020**, *370* (6520), eabd4250.
- (29) Zhang, Y.; Zeng, G.; Pan, H.; Li, C.; Hu, Y.; Chu, K.; Han, W.; Chen, Z.; Tang, R.; Yin, W.; Chen, X.; Hu, Y.; Liu, X.; Jiang, C.; Li, J.; Yang, M.; Song, Y.; Wang, X.; Gao, Q.; Zhu, F. Safety, Tolerability, and Immunogenicity of an Inactivated SARS-CoV-2 Vaccine in Healthy Adults Aged 18–59 Years: A Randomised, Double-Blind, Placebo-Controlled, Phase 1/2 Clinical Trial. *Lancet Infect. Dis.* **2021**, *21* (2), 181–192.
- (30) Yang, H. S.; Costa, V.; Racine-Brzostek, S. E.; Acker, K. P.; Yee, J.; Chen, Z.; Karbaschi, M.; Zuk, R.; Rand, S.; Sukhu, A.; Klasse, P. J.; Cushing, M. M.; Chadburn, A.; Zhao, Z. Association of Age With SARS-CoV-2 Antibody Response. *JAMA Netw. Open* **2021**, *4* (3), e214302.
- (31) Gudbjartsson, D. F.; Norddahl, G. L.; Melsted, P.; Gunnarsdottir, K.; Holm, H.; Eythorsson, E.; Arnthorsson, A. O.; Helgason, D.; Bjarnadottir, K.; Ingvarsson, R. F.; Thorsteinsdottir, B.; Kristjansdottir, S.; Birgisdottir, K.; Kristinsdottir, A. M.; Sigurdsson, M. I.; Arnadottir, G. A.; Ivarsdottir, E. V.; Andresdottir, M.; Jonsson, F.; Agustsdottir, A. B.; Berglund, J.; Eiriksdottir, B.; Fridriksdottir, R.; Gardarsdottir, E. E.; Gottfredsson, M.; Gretarsdottir, O. S.; Gudmundsdottir, S.; Gudmundsson, K. R.; Gunnarsdottir, T. R.; Gylfason, A.; Helgason, A.; Jenson, B. O.; Jonasdottir, A.; Jonsson, H.; Kristjansson, T.; Kristinsson, K. G.; Magnúsdottir, D. N.; Magnússon, O. T.; Olafsdottir, L. B.; Rognvaldsson, S.; le Roux, L.; Sigmundsdottir, G.; Sigurdsson, A.; Sveinbjornsson, G.; Sveinsdottir, K. E.; Sveinsdottir, M.; Thorarensen, E. A.; Thorbjornsson, B.; Thordardottir, M.; Saemundsdottir, J.; Kristjansson, S. H.; Josefsdottir, K. S.; Masson, G.; Georgsson, G.; Kristjansson, M.; Moller, A.; Palsson, R.; Gudnason, T.; Thorsteinsdottir, U.; Jonsdottir, I.; Sulem, P.; Stefansson, K. Humoral Immune Response to SARS-CoV-2 in Iceland. *N. Engl. J. Med.* **2020**, *383* (18), 1724–1734.
- (32) Emami, A.; Javanmardi, F.; Pirbonyeh, N.; Akbari, A. Prevalence of Underlying Diseases in Hospitalized Patients with COVID-19: A Systematic Review and Meta-Analysis. *Arch. Acad. Emerg. Med.* **2020**, *8* (1), e35.
- (33) Robbiani, D. F.; Gaebler, C.; Muecksch, F.; Lorenzi, J. C. C.; Wang, Z.; Cho, A.; Agudelo, M.; Barnes, C. O.; Gazumyan, A.; Finkin, S.; Hägglöf, T.; Oliveira, T. Y.; Viant, C.; Hurley, A.; Hoffmann, H.-H.; Millard, K. G.; Kost, R. G.; Cipolla, M.; Gordon, K.; Bianchini, F.; Chen, S. T.; Ramos, V.; Patel, R.; Dizon, J.; Shimeliovich, I.; Mendoza, P.; Hartweg, H.; Nogueira, L.; Pack, M.; Horowitz, J.; Schmidt, F.; Weisblum, Y.; Michailidis, E.; Ashbrook, A. W.; Waltari, E.; Pak, J. E.; Huey-Tubman, K. E.; Koranda, N.; Hoffman, P. R.; West, A. P., Jr; Rice, C. M.; Hatziioannou, T.; Bjorkman, P. J.; Bieniasz, P. D.; Caskey, M.; Nussenzweig, M. C. Convergent Antibody Responses to SARS-CoV-2 in Convalescent Individuals. *Nature* **2020**, *584* (7821), 437–442.
- (34) Liu, Y.; Wang, K.; Massoud, T. F.; Paulmurugan, R. SARS-CoV-2 Vaccine Development: An Overview and Perspectives. *ACS Pharmacol. Transl. Sci.* **2020**, *3* (5), 844–858.
- (35) Jeyanathan, M.; Afkhami, S.; Smail, F.; Miller, M. S.; Lichty, B. D.; Xing, Z. Immunological Considerations for COVID-19 Vaccine Strategies. *Nat. Rev. Immunol.* **2020**, *20* (10), 615–632.
- (36) Udugama, B.; Kadhiresan, P.; Chan, W. C. W. Tunable and Precise Miniature Lithium Heater for Point-of-Care Applications. *Proc. Natl. Acad. Sci. U. S. A.* **2020**, *117* (9), 4632–4641.
- (37) Salath, M.; Althaus, C.; Anderegg, N.; Antonioli, D.; Ballouz, T.; Bugnon, E.; apkun, S.; Jackson, D.; Kim, S.-I.; Larus, J.; Low, N.; Lueks, W.; Menges, D.; Moullet, C.; Payer, M.; Riou, J.; Stadler, T.; Troncoso, C.; Vayena, E.; von Wyl, V. Early Evidence of Effectiveness of Digital Contact Tracing for SARS-CoV-2 in Switzerland. *Swiss. Med. Wkly.* **2020**, *150*, w20457.